2013 IEEE 10th International Symposium on Biomedical Imaging:
From Nano to Macro
San Francisco, CA, USA, April 7-11, 2013

LABELING WHITE MATTER TRACTS IN HARDI BY FUSING MULTIPLE TRACT ATLASES WITH APPLICATIONS TO GENETICS

Yan Jin[1], Yonggang Shi[1], Liang Zhan[1], Greig I. de Zubicaray[2], Katie L. McMahon[2], Nicholas G. Martin[3], Margaret J. Wright[3], Paul M. Thompson[1]

[1] Imaging Genetics Center, Lab of Neuro Imaging, UCLA School of Medicine, Los Angeles, CA 90095, USA
[2]University of Queensland, Brisbane St. Lucia, QLD 4072, Australia
[3]Queensland Institute of Medical Research, Herston, QLD 4029, Australia

ABSTRACT

Accurate identification of white matter structures and segmentation of fibers into tracts is important in neuroimaging and has many potential applications. Even so, it is not trivial because whole brain tractography generates hundreds of thousands of streamlines that include many false positive fibers. We developed and tested an automatic tract labeling algorithm to segment anatomically meaningful tracts from diffusion weighted images. Our multi-atlas method incorporates information from multiple hand-labeled fiber tract atlases. In validations, we showed that the method outperformed the standard ROI-based labeling using a deformable, parcellated atlas. Finally, we show a high-throughput application of the method to genetic population studies. We use the sub-voxel diffusion information from fibers in the clustered tracts based on 105-gradient HARDI scans of 86 young normal twins. The whole workflow shows promise for larger population studies in the future.

Index Terms— HARDI, Tractography, Fiber Clustering, Label Fusion, Genetic Heritability

1. INTRODUCTION

Diffusion weighted MR imaging (DWI) is increasingly used to study pathology and connectivity of the white matter (WM) pathways in the living brain. Recently, more advanced diffusion imaging models such as high angular resolution diffusion imaging (HARDI [1]) and diffusion spectrum imaging have been more widely adopted, as they offer the angular resolution needed to resolve fibers that mix and cross. Tractography can fit a path through the directional diffusion data at each voxel, generating hypothetical streamlines that are inferred to represent neural pathways throughout the whole volume of brain.

However, the results of whole-brain tractography are too complex and cluttered to be interpretable without further analysis to organize or group the extracted fibers. Clustering – extracting anatomically meaningful sets of streamlines, or tracts – is also a useful step in defining regional connectivity and in measuring fiber integrity for coherent fiber pathways. Intuitively, anatomically well-known WM tracts can be extracted based on ROI constraints obtained by a parcellated volumetric atlas or manual tracing [2]. The advantage of this approach is that the resulting sets of streamlines can be fed into large-scale population studies [3], but the final results often need manual intervention to screen out false positive fibers.

A classic automatic clustering framework calculates a pairwise similarity metric (e.g., distance) between all pairs of fibers and the resulting matrix is fed into standard clustering algorithms to separate them into distinct bundles [4]. However, without anatomical guidance, clustering results heavily rely on the number of clusters a user decides empirically. In "bottom-up" methods, major tracts emerge by adding up smaller groups hierarchically, starting from individual fibers. This may not efficiently filter out erroneous fibers buried among the large number of streamlines (100,000-1,000,000) that whole-brain tractography generates. Recent hybrid approaches [5] extract the well-known WM tracts by combining prior information from an atlas with data-driven similarity-based clustering. However, it is not yet clear how best to pick an atlas that can successfully find fibers in new scans, adapting to the large individual tract variability, which is itself of interest in large-scale group studies.

In [6], we introduced a *multi-atlas label fusion* framework to automatically extract anatomically meaningful WM tracts. Our "top-down" approach produced hand-made multiple WM tract atlases as guidance and a distance metric to screen trajectories for tracts of interest. We then used a label fusion scheme, which has been well-established in traditional intensity-based image segmentation [7], to fuse the clustered results obtained from individual atlases. In this work, we further refine our algorithm as follows: 1) Probabilistic tractography is implemented to increase the quality and the number of fibers; 2) More anatomically well-known tracts are included in the hand-made atlases; 3) ROI constraints are added to assist clustering; 4) Label fusion scheme includes distance consideration over simple majority voting; 5) Quantitative validation is carefully done

against manual segmentation; 6) We design a pointwise fiber correspondence matching approach across the population and gather their diffusion properties in a genetic heritability application to demonstrate how to apply the sub-voxel fiber information to a real biological question.

2. LABEL CLUSTERING & FUSION

2.1. Tractography

We performed whole brain tractography with Camino (http://cmic.cs.ucl.ac.uk/camino/). We used Probabilistic Index of Connectivity (PICo) tractography [8], to follow the principal diffusion directions obtained by spherical harmonic reconstruction of the HARDI data to generate fibers throughout the entire brain.

2.2. WM Tract Atlas Construction

We constructed seven WM tract atlases, from 7 randomly chosen normal subjects from our HARDI dataset. The fractional anisotropy (FA) images of all the atlases were registered to a single-subject template in the ICBM-152 space called the "Type II Eve Atlas" (a 32-year old healthy female) [9]. The entire brain of the "Eve" template was parcellated using 130 bilateral ROIs.

The labeled template ROIs were re-assigned to the seven registered atlases, respectively, by warping them with the deformation fields generated by Advanced Neuroimaging Tools (ANTs) (http://www.picsl.upenn.edu/ANTS/). Fibers that traversed the ROIs were extracted according to the lookup table in [10]. For example, the corticospinal tract was extracted from fibers passing between the precentral gyrus and cerebral peduncle. In creating the atlases, each tract was manually edited to remove visible outliers.

Currently, each atlas is comprised of 17 major WM tracts (but could be further supplemented in the future): left/right corticospinal tract (CST), left/right anterior thalamic radiation (ATR), left/right cingulum (CGC), left/right inferior fronto-occipital fasciculus (IFO), left/right inferior longitudinal fasciculus (ILF), left arcuate fasciculus (part of the superior longitudinal fasciculus) (ARC), and six segments of the corpus callosum – projecting to both frontal lobes (CC-FRN), precentral gyri (CC-PRC), postcentral gyri (CC-POC), superior parietal lobes (CC-PAR), temporal lobes (CC-TEM), and the occipital lobes (CC-OCC). We did not include the right arcuate fasciculus because not everyone has a complete instance of this tract [11], which leads to difficulties in performing statistical analysis. **Figure 1** shows an example of the WM tract atlases that we created (*back, left side,* and *bottom* views).

2.3. Fiber Clustering

Using Camino, we extracted whole-brain tractography from additional subjects whose WM fibers need to be clustered and labeled. Then, the labeled "Eve" template ROIs were re-assigned to the subject through registration. Based on the look-up table in [10], those fibers that did not traverse the ROIs for a particular tract were filtered out. This reduced the fiber count for a given tract from a million to a few hundreds or thousands.

Next, the same registration transform was used to align the subject's FA image to each of the seven WM tract atlases' FA images, respectively. Each atlas's tracts were warped to the subject space with the corresponding deformation fields generated from the FA registration. Scalar registration is preferred than ODF-based registration under the multi-atlas scenario because it reduces computing time significantly (from a few hours per subject to around 5 minutes for our dataset) and computing resources in population studies. Moreover, fiber alignment is indeed improved significantly with FA registration [12].

We defined a fiber distance metric to decide which fibers from each subject should be included in any individual warped atlas tract, based on an empirical threshold (15mm for our dataset). For any pair of fibers γ_i and γ_j, we define the symmetric Hausdorff distance [4]: $d_H(\gamma_i,\gamma_j) = \max(d_{H'}(\gamma_i,\gamma_j), d_{H'}(\gamma_j,\gamma_i))$, where $d_{H'}$ is the asymmetric Hausdorff distance. $d_{H'}(\gamma_i,\gamma_j) = max_{x\epsilon\gamma i}\ min_{y\epsilon\gamma j}\ \|x - y\|$. $\|.\|$ is the Euclidean norm and the ordered pair (γ_i,γ_j) indicates an asymmetric distance from γ_i to γ_j. Here the x's and y's are the coordinate points along fibers γ_i and γ_j, respectively.

For each fiber member of a particular tract in an atlas, we computed the distance between this fiber and each remaining fiber that survived the ROI constraints in the subjects' tractography. The subject's fibers whose distances are less than the threshold were considered candidates for that particular tract.

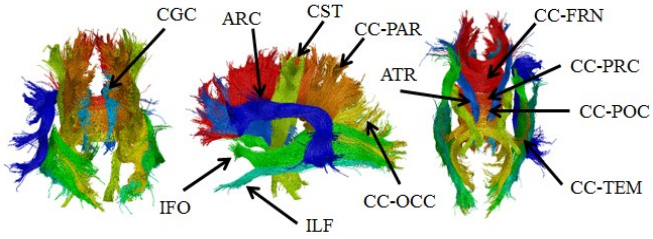

Figure 1. A representative WM fiber atlas computed, and manually edited, from 4-Tesla 105-gradient HARDI data, showing major tracts. We created these, with manual editing, in 7 subjects, and they are then propagated into new subjects. *Back*, *left side*, and *bottom* views are shown.

2.4. Label Fusion

We chose the Hausdorff distance metric in the fiber clustering phase to ensure that only streamlines were selected that had similar geometric shapes, and that lay in the region where the particular atlas WM tract is located. However, due to shape variability among individual WM atlases, often the same tract in multiple atlases might nominate different candidates based on its own shape. We

defined a mean fiber distance metric to rank the fibers nominated by individual atlases. For each fiber, D_{mean}=(the sum of the Hausdorff distances from the nominated atlases+ empirical cutoff threshold*the number of non-nominated atlases)/total number of atlases. An empirical percentage threshold was used to decide how many fibers were included in the final result for each particular tract.

3. GENETIC HERITABILITY ANALYSIS

3.1. Fiber Matching

To perform group studies, we need to establish a point-wise correspondence between fibers of the segmented tracts across the population. To be more precise, for each particular tract, we choose a representative sample among our manually constructed atlases. For each point on the fibers that belong to this tract, we warped it to each subject in the rest of the population by applying the deformation field obtained in **Section 2.3**. Next, we located all fibers of that tract in that subject within a neighborhood (a sphere with the radius of 1.5 voxel) of the warped atlas point. Finally, we chose the projection point on the fiber that had the shortest projection distance from the warped atlas point as the "corresponding" point in that subject. If no fibers fall into the neighborhood of the warped atlas point, we would just use the warped atlas point as the "corresponding" point. An illustration of fiber matching is shown in **Figure 2**.

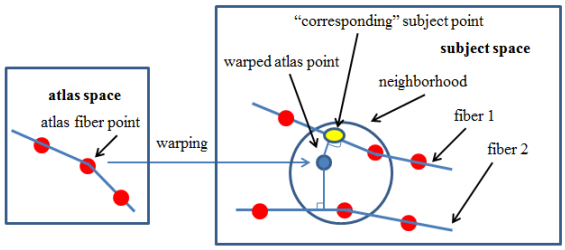

Figure 2. An illustration of how to choose a "corresponding" fiber point in a subject.

3.2. Genetic Analysis

Monozygotic (MZ) twins share 100% of their genetic variants whereas dizygotic (DZ) twins share, on average 50%, of their genetic polymorphisms. A simple and widely-used estimate of heritability (proportion of variance due to genetic factors), in twin studies, assesses how much the intra-class correlation for MZ twin pairs (r_{MZ}) exceeds the DZ twin correlation (r_{DZ}). Falconer's heritability statistic [13] is defined as $h^2=2(r_{MZ}-r_{DZ})$. It estimates the proportion of the overall variance that is due to genetic differences among individuals. More complex methods exist to estimate heritability, but we use Falconer's here just as an example. Interpolated FA values at "corresponding" fiber points of a particular tract across the population were used to calculate intra-class correlations r_{MZ} and r_{DZ}, and h^2.

3.3. Subjects and Image Acquisition

For this study we included data from 86 healthy, right-handed, young adult twins from 43 families in Australia with 22 same-sex MZ twin pairs (11 male pairs) and 21 same-sex DZ pairs (9 male pairs). Each image volume consisted of 55 1.79x1.79x2mm axial slices. 105 DWI volumes were acquired per subject: 11 T2-weighted b_0 image volumes and 94 diffusion-weighted volumes (b = 1159 s/mm^2).

4. RESULTS

4.1. Clustering Visualization

Figure 3 shows how we obtained the left arcuate in a test subject. The first row shows the atlas versions of the tract. The second row shows the different candidates for this tract in the same test subject, based on using each atlas to decide which fibers it should contain. The final result for this tract was obtained by applying the label fusion scheme in **Section 2.4**. The manual segmentation result is also included for comparison (see the *right bottom panel*).

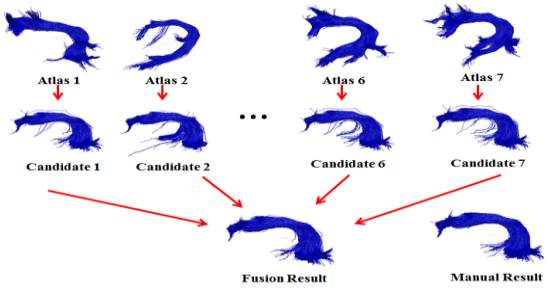

Figure 3. Label fusion result for the left arcuate fasciculus (in *blue*) in a test subject (viewed from the *left*).

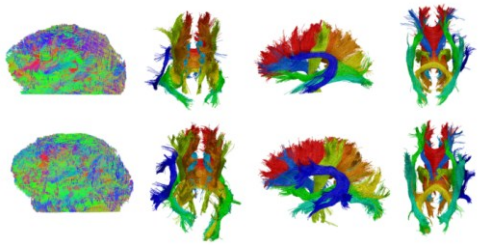

Figure 4. *Back*, *left side*, and *bottom* views of two subjects' fiber clustering are shown. The original whole brain tractography (*leftmost column*) is included for comparison, clearly showing the utility of the data reduction.

Figure 4 shows automatic WM fiber clustering results for two representative test subjects. *Back*, *left side*, and *bottom* views are shown. The types of tracts and their colors are as in **Figure 1**.

4.2. Quantitative Validation

To quantitatively evaluate the proposed framework, we first

converted each of the fiber tracts to a binary image, where voxels that the tracts cross are marked as 1, and 0 otherwise. Then the *Dice coefficient* of two tracts is defined as: $D(a,b)=2(V(a) \cap V(b))/(V(a)+V(b))$, where V() is the voxel volume the tract penetrates.

We randomly selected 8 subjects (no twin pairs) from our twin datasets. And we performed leave-one-out cross validation, i.e., using 7 subjects as atlases to test on the 8th one. **Figure 5** shows the average Dice coefficients for all tracts mentioned in **Section 2.2** with our label fusion method and ROI-only clustering (based on the look-up table in [10]) against manual segmentation (ground truth).

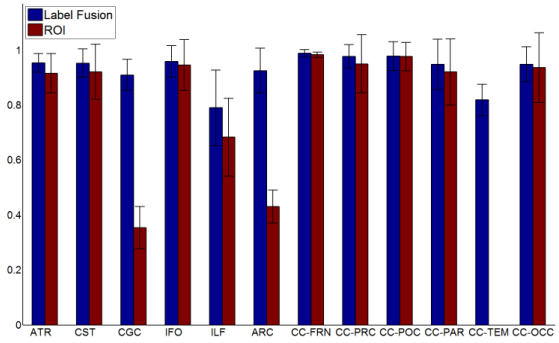

Figure 5. The average Dice coefficients and standard errors (error bars) of all the tracts described in **Section 2.2** for our label fusion method and the ROI method against manual segmentation.

How many atlases are needed is still an open question. However, based on the Dice coefficients, 7 atlases may well capture the variability, at least for our dataset. Overall, our algorithm outperformed the ROI method for every tract, and also gave a smaller variance, especially on those tracts that have unclear or no ROI constraints (CGC, ARC, ILF and CC-TEM). As to the fusion percentage, we chose 20%-50% for those tracts with unclear or no ROI constraints and 80%-100% otherwise.

4.3. Falconer Heritability

Figure 6 shows the Falconer heritability statistic based on the FA values for two different segmented tracts (left CST and left IFO) based on 76 twins after for correcting multiple comparisons using the false discovery rate method (p=0.05). Higher Falconer statistics suggest genetic influences on those parts of tracts (h^2~1).

5. CONCLUSION

Here we extended the label fusion concept to fiber clustering and compared it to an automatic ROI-based method for quantitative validation. We also showed an example of how to perform a group statistical analysis (here, a heritability study) by using the sub-voxel fiber diffusion information mapped onto the clustered tracts. This complete workflow provides us with a practical tool for future large population studies that may reveal how the brain is affected by genetic factors, and by a variety of psychiatric or neurological disorders such as Alzheimer's disease.

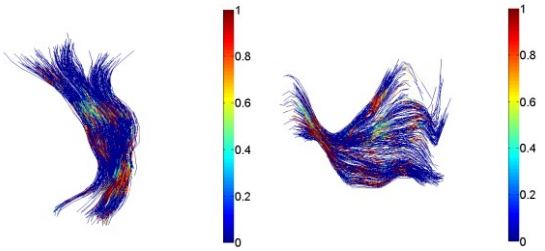

Figure 6. Color maps show example maps of Falconer's heritability statistic for the left corticospinal tract (*left*) and left inferior fronto-occipital fasciculus (*right*).

6. ACKNOWLEDGEMENTS

This study was supported by Grant R01HD050735, K01EB013633, and P41EB015922 from NIH and Grant 496682 from NHMRC, Australia.

7. REFERENCES

[1] D.S. Tuch, "Q-Ball Imaging," *Magnetic Resonance in Medicine*, 52, pp. 1358-1372, 2004.

[2] S. Wakana *et al.*, "Reproducibility of Quantitative Tractography Methods Applied to Cerebral White Matter," *NeuroImage*, 36, pp. 630-644, 2007.

[3] P.A.Yushkevich *et al.*, "Structure-specific Statistical Mapping of White Matter Tracts," *NeuroImage*, 41, pp. 448-461, 2008.

[4] L.J. O'Donnell and C.F. Westin, "Automatic Tractography Segmentation Using a High-dimensional White Matter Atlas," *IEEE Transactions on Medical Imaging*, 26, pp. 1562-1575, 2007.

[5] P. Guevara *et al.*, "Automatic Fiber Bundle Segmentation in Massive Tractography Datasets Using a Multi-subject Bundle Atlas," *NeuroImage*, 61, pp. 1083-1099, 2012.

[6] Y. Jin *et al.*, "Automatic Population HARDI White Matter Tract Clustering by Label Fusion of Multiple Tract Atlases," In: 15th MICCAI Mutimodal Brain Image Analysis Workshop, 2012.

[7] M.R. Sabuncu *et al.*, "A Generative Model for Image Segmentation Based on Label Fusion," *IEEE Transactions on Medical Imaging*, 29, pp. 1714-1729, 2010.

[8] G.J.M. Parker *et al.*, "A Framework for a Streamline-based Probabilistic Index of Connectivity (PICo) Using a Structural Interpretation of MRI Diffusion Measurements," *Magnetic Resonance Imaging*, 18, pp.242-254, 2003.

[9] K. Oishi *et al.*, "Atlas-based Whole Brain White Matter Analysis Using Large Deformation Diffeomorphic Metric Mapping: Application to Normal Elderly and Alzheimer's Disease Participants," *NeuroImage*, 46, pp. 486-499, 2009.

[10] Y. Zhang *et al.*, "Atlas-Guided Tract Reconstruction for Automated and Comprehensive Examination of the White Matter Anatomy," *NeuroImage*, 52, pp. 1289-1301, 2010.

[11] M. Catani *et al.*, "Symmetries in Human Brain Language Pathways Correlate with Verbal Recall," *Proceedings of the National Academy of Sciences*, 104, pp. 17163-17168, 2007.

[12] Y. Jin *et al.*, "3D Elastic Registration Improves HARDI-derived Fiber Alignment and Automated Tract Clustering," In: *8th IEEE ISBI*, pp. 822-826, 2011.

[13] D. Falconer and T.F. Mackay, "*Introduction to Quantitative Genetics*," 4th ed., Benjamin Cummings, 1996.